

# The influence of a metallic sheet on an evanescent mode atomic mirror

J. B. Kirk\*, C. R. Bennett<sup>†</sup>, M. Babiker<sup>†</sup> and S. Al-Awfi<sup>††</sup>

\* Department of Physics, University of Essex, Colchester, Essex CO4 3SQ, UK

<sup>†</sup> Department of Physics, University of York, Heslington, York, YO10 5DD, UK

<sup>††</sup> Department of Physics, King Abdulaziz University, P O Box 344, Medina, Saudi-Arabia

## Abstract

A theory of evanescent mode atomic mirrors utilising a metallic sheet on a dielectric substrate is described. The emphasis here is on the role of the metallic sheet and on the evaluation of atomic trajectories using the field-dipole orientation picture. At low intensity, the atomic reflection process is controlled by two separate mechanisms both of which are modified by the presence of the metallic sheet and influenced by the use of the field-dipole orientation picture. The first mechanism involves the spontaneous force which accelerates the atom parallel to the sheet plane. The second mechanism involves the combined dipole plus van der Waals force which acts to repel the atom from the surface, decelerating its motion until it attains an instantaneous halt before changing direction away from the surface at an appropriate turning point in the trajectory. Various quantitative features arising from varying the controllable parameters of the system, including screening effects as well as desirable enhancement effects, are pointed out and discussed.

**PACS numbers:** 42.50.Vk, 32.70.Jz, 32.80.Pj, 32.80.Lg

One of the primary aims, yet to be fully accomplished in the rapidly developing field of atom optics is the standardisation of the atomic mirror as a routine atom optical element. The idea of an atomic mirror, a device capable of reflecting atoms, was first put forward by Cooke and Hill in 1982 [1]. Since then, a number of studies, both theoretical and experimental, have sought to explore various aspects of atomic mirrors, based on different mechanisms of atom reflection from planar surfaces [2-19]. In particular, the evanescent mode atomic mirror is suitable for neutral atoms undergoing electric dipole transitions [14,18,19]. The mechanism in this type of mirror makes use of light evanescing into the vacuum region outside the planar surface of a dielectric when laser light is internally reflected. The evanescent light sets up a repulsive dipole potential which acts on any neutral atom possessing a transition frequency at near resonance with, and blue-detuned from, the laser frequency. The limiting factors of such a mirror stem primarily from heating effects and also from fluctuations due to the light which become negligible at low intensities. A device operating at low intensities was thus needed. This was the motivation behind the studies which highlight the role of a thin metallic layer deposited on the surface in providing an enhancement of the evanescent component [18,19].

The purpose of this article is to report a theory of evanescent mode atomic mirrors with a metallic sheet, exploring the nature of the enhancement, determining the general features of the mirror and evaluating the trajectories for a typical set of parameters.

It turns out that a quantitative theoretical analysis demands the implementation of a number of steps. First, a mode normalisation procedure in terms of intensity is needed for the incident light mode responsible for the generation of the evanescent component. Secondly, the jump conditions should be implemented involving the surface current arising from the finite two-dimensional conductivity of the metallic sheet. Thirdly, the attractive force between the atom and the dielectric in the presence of the metallic sheet should be included in the dynamics to determine the trajectories. Finally, use

should be made of the field-dipole orientation picture for evaluating the radiation forces as well as the van der Waals-type atom-surface force. The role of the field-dipole orientation picture is to determine an average value for the local orientation of the electric dipole moment vector in the presence of the evanescent field. We show here that a programme incorporating the above theoretical features permits the atomic trajectories to be determined by direct solution of the equation of motion, leading either to a reflection of the atom off the mirror or a collision with it, in a manner dependent on the chosen set of parameters. Existing treatments determining trajectories are primarily based on Monte Carlo techniques.

The basic elements comprising the atomic mirror are shown schematically in Fig. 1. Here a metallic sheet in the form of an infinitesimally thin layer is deposited on the planar surface of a dielectric substrate (or glass prism). Light of frequency  $\omega$  incident from within the dielectric is internally reflected at the interface between the dielectric substrate and the metallic sheet. This creates a field in the vacuum region which is decaying with distance from the metallic sheet and is propagating along the surface. A neutral atom possessing a transition frequency  $\omega_0 < \omega$  and which is moving in the plane of incidence would be subject to the repulsive dipole force plus an attractive atom-surface force and will also experience a light pressure force parallel to the surface. As we show below the combined influence of these forces can be made to control the reflection process.

The relevant electric field vector at frequency  $\omega$  can be written in terms of incident (I), reflected (R) and evanescent (1) parts as follows

$$\mathbf{E}(\mathbf{r}, t) = \left\{ \left( \mathbf{E}_I(\mathbf{k}_{\parallel}, \mathbf{r}, t) + \mathbf{E}_R(\mathbf{k}_{\parallel}, \mathbf{r}, t) \right) \theta(-z) + \mathbf{E}_1(\mathbf{k}_{\parallel}, \mathbf{r}, t) \theta(z) \right\} a + h.c. \quad (1)$$

where  $\theta$  is the unit step function and the fields are given by

$$\mathbf{E}_I(\mathbf{k}_{\parallel}, \mathbf{r}, t) = A_I \left( 1, 0, -\frac{k_{\parallel}}{k_{z2}} \right) e^{ik_{z2}z} e^{i(\mathbf{k}_{\parallel} \cdot \mathbf{r}_{\parallel} - \omega t)} \quad (2)$$

$$\mathbf{E}_R(\mathbf{k}_{\parallel}, \mathbf{r}, t) = A_R \left( 1, 0, \frac{k_{\parallel}}{k_{z2}} \right) e^{-ik_{z2}z} e^{i(\mathbf{k}_{\parallel} \cdot \mathbf{r}_{\parallel} - \omega t)} \quad (3)$$

$$\mathbf{E}_1(\mathbf{k}_{\parallel}, \mathbf{r}, t) = B \left( 1, 0, \frac{ik_{\parallel}}{k_{z1}} \right) e^{-k_{z1}z} e^{i(\mathbf{k}_{\parallel} \cdot \mathbf{r}_{\parallel} - \omega t)} \quad (4)$$

Here  $\mathbf{k}_{\parallel}$  is the wavevector parallel to the surface. Its magnitude  $k_{\parallel}$  is given by  $c^2 k_{\parallel}^2 = \omega^2 \epsilon_2 \sin^2 \phi$  where  $\phi$  is the angle of incidence. The three quantities between the brackets in each of Eqs.(2) to (4) stand for the vector components parallel to  $\mathbf{k}_{\parallel}$ , perpendicular to it on the surface plane and along the z-direction, respectively.  $k_{z1}$  and  $k_{z2}$  (both real) are defined by

$$k_{z1}^2 = k_{\parallel}^2 - \frac{\epsilon_1 \omega^2}{c^2} > 0; \quad k_{z2}^2 = \frac{\epsilon_2 \omega^2}{c^2} - k_{\parallel}^2 > 0 \quad (5)$$

Finally,  $A_I, A_R$  and  $B$  are field amplitude factors, to be determined. The notation is such that parameters associated with the substrate are labelled by the subscript 2, while for the outer region (vacuum) the label is 1. Both dielectric functions  $\epsilon_1$  and  $\epsilon_2$  are assumed to be frequency-independent and we take  $\epsilon_1 = 1$ , as appropriate for vacuum. The position vector is written as  $\mathbf{r} = (\mathbf{r}_{\parallel}, z)$  in terms of an in-plane position vector  $\mathbf{r}_{\parallel}$  and a z-coordinate relative to the metallic sheet. The role of the metallic sheet is primarily to provide a two-dimensional charge density  $n_s$  and, so, an electrical conductivity  $in_s e^2 / m^* (\omega + i\gamma)$  where  $m^*$  and  $e$  are the electronic effective mass and charge and  $\gamma \ll \omega$  accounts for metallic plasma loss effects. The metallic sheet only enters the formalism via the electromagnetic boundary conditions involving the tangential components of the magnetic fields corresponding to Eqs.(2) to (4), which can be calculated using Maxwell's equation  $\mathbf{H} = -(i\epsilon_0 c^2 / \omega) \nabla \times \mathbf{E}$ . Application of the first boundary condition, namely the continuity of the tangential component of the electric field vector at  $z = 0$ , yields

$$A_I + A_R = B \quad (6)$$

The second electromagnetic boundary condition is that the tangential component of the magnetic field vector experiences a discontinuity at  $z = 0$  arising from the surface

current induced by the in-plane component of the electric field at the metallic sheet.

We have

$$H_{\parallel}(0_-) - H_{\parallel}(0_+) = \frac{in_s e^2}{m^*(\omega + i\gamma)} E_{\parallel}(0) \quad (7)$$

where  $0_{\pm}$  are the limits as  $\xi \rightarrow 0$  of  $(0 \pm \xi)$ . Application of this boundary condition leads to a second relation connecting the field amplitudes

$$\frac{\epsilon_2}{k_{z2}} (A_I - A_R) + i \frac{\epsilon_1}{k_{z1}} B = \frac{in_s e^2}{\epsilon_0 m^* \omega (\omega + i\gamma)} \quad (8)$$

Elimination of  $A_R$  between Eqs.(6) and (8) yields straightforwardly

$$B = 2A_I \left[ i \frac{k_{z2}}{\epsilon_2} \left( \frac{n_s e^2}{\epsilon_0 m^* \omega (\omega + i\gamma)} - \frac{\epsilon_1}{k_{z1}} \right) + 1 \right]^{-1} \quad (9)$$

The next step is to determine the value for the amplitude  $A_I$ . This is the amplitude of the incident field in the unbounded bulk of material 2 and the value of  $A_I$  is such that the Hamiltonian  $\mathcal{H}_I$  reduces to the canonical form

$$\mathcal{H}_I = \frac{\epsilon_0}{2} \int d\mathbf{r} \left\{ \epsilon_2 E_I^2 + \frac{1}{(\epsilon_0 c)^2} H_I^2 \right\} = \frac{1}{2} \hbar \omega (aa^\dagger + a^\dagger a) \quad (10)$$

Thus we find

$$A_I^2 = \frac{\hbar k_{z2}^2 c^2}{2V \epsilon_0 \epsilon_2^2 \omega} \quad (11)$$

where  $V$  is the (large) volume of material 2.

The average radiation force acting on an atom of transition frequency  $\omega_0$  moving in the vacuum region at velocity  $\mathbf{v}$  is given by the well known expression [20,22]

$$\mathbf{F}(\mathbf{r}, \mathbf{v}) = 2\hbar \left\{ \frac{\Gamma \Omega_R^2 \mathbf{k}_{\parallel} - \frac{1}{2} \Delta \nabla \Omega_R^2}{\Delta^2 + 2\Omega_R^2 + \Gamma^2} \right\} = \mathbf{F}_s + \mathbf{F}_d \quad (12)$$

where  $\mathbf{F}_s$  corresponds to the first term, identified as the spontaneous force along the wave propagation direction  $\mathbf{k}_{\parallel}$ , and  $\mathbf{F}_d$  corresponds to the second term, identified as the dipole force;  $\Delta$  is the dynamic detuning given by

$$\Delta = \Delta_0 - \mathbf{k}_{\parallel} \cdot \mathbf{v} \quad (13)$$

with  $\Delta_0 = \omega - \omega_0$  the static detuning of the light from the atomic resonance. The force given in Eq.(12) is applicable in the low intensity limit for which the saturation

parameter  $S$  satisfies the inequality  $S = 2\Omega_R^2/(\Delta^2 + \Gamma^2) < 1$ , where  $\Omega_R(0)$  is the Rabi frequency, defined below, evaluated at  $z = 0$ , and  $\Gamma$  is the spontaneous emission rate. At the high intensity regime, corresponding to  $S \gg 1$  one needs to adopt the dressed atom approach [21]. The low intensity regime is the correct regime in the context of the atomic mirrors considered here for which it can readily be verified that  $S < 1$ , so that the dynamics based on the average radiation forces given by Eq.(12) is applicable.

Of the two average radiation forces, it is easy to see that  $\mathbf{F}_d$  can act as a repulsive force provided that the detuning  $\Delta_0$  is positive (blue detuning). Note that  $\mathbf{v}$ , the velocity of the atom, is in the plane of incidence as in Fig. 1, i.e. has only two components, a z-component and a component parallel to  $\mathbf{k}_\parallel$ . The Rabi frequency  $\Omega_R$  entering Eq.(12) is defined for the electric dipole  $\boldsymbol{\mu}$  in the evanescent field  $\mathbf{E}_1(\mathbf{k}_\parallel, \mathbf{r}, t)$

$$\Omega_R = \left| \frac{\alpha \boldsymbol{\mu} \cdot \mathbf{E}_1(\mathbf{k}_\parallel, \mathbf{r}, t)}{\hbar} \right| \quad (14)$$

where  $\alpha$  is a complex amplitude factor such that  $a \rightarrow \alpha$  in the classical electromagnetic field limit. It is in fact related to the intensity  $I$  of the incident beam by the well known relation [23]

$$|\alpha|^2 = \frac{IV}{\hbar c \omega} \quad (15)$$

It can be seen from Eq.(4) that the evanescent field possesses two vector components. However, once the evanescent field has been set up, the average atomic dipole moment vector at any given point aligns itself along, and follows the oscillations of, the local evanescent electric field vector. The appropriate Rabi frequency in this field-dipole orientation picture is thus given by [22]

$$\hbar \Omega_R(\mathbf{r}) = |\alpha| \mu E_1(\mathbf{r}) \quad (16)$$

where  $\mu$  and  $E_1$  are the magnitudes of these vectors. Using Eqs.(4) and (9) we can write the square of the Rabi frequency in the limit  $\gamma \rightarrow 0$  in the following form, emphasising the dependence on the angle of incidence  $\phi$ , which is related to  $k_\parallel$  through

$$c^2 k_{\parallel}^2 = \omega^2 \epsilon_2 \sin \phi,$$

$$\Omega_R^2(\omega, \phi, z) = \frac{4|\alpha|^2 \mu^2 k_{z2}^2 c^2 e^{-2k_{z1}z}}{2\hbar V \epsilon_0 \epsilon_2^2 \omega} \left[ 1 + \frac{k_{z2}^2 \epsilon_1^2}{k_{z1}^2 \epsilon_2^2} \left( \frac{\Lambda^2 k_{z1} d}{\omega^2} - 1 \right)^2 \right]^{-1} (1 + k_{\parallel}^2 / k_{z1}^2) \quad (17)$$

where  $\Lambda$  is a convenient scaling frequency defined by

$$\Lambda^2 = \frac{n_s e^2}{m^* \epsilon_0 \epsilon_1 d} \quad (18)$$

with  $d$  a convenient scaling length. Note the presence of the second term in the expression between the last pair of brackets in Eq.(17) which is proportional to  $k_{\parallel}^2 / k_{z1}^2$ . This represents the contribution from the z-component of  $\mathbf{E}_1$ , and since  $k_{z1}$  can be very small (when the angle of incidence is close to the total internal reflection angle), this could lead to an enhancement, in contrast to the contribution from the in-plane component (corresponding to the first term in the last pair of bracket in Eq.(17)) which does not exhibit this feature.

Figure 2 displays the effects of varying the sheet electron density  $n_s$  on the value of the squared Rabi frequency  $\Omega_R^2(\omega, \phi, 0)$ , i.e. evaluated at the surface  $z = 0$ . This quantity provides an indication of the effectiveness of the structure as an atomic mirror. The curves correspond to different values of angle of incidence  $\phi$ . There are two features worthy of note here. First, for a given  $\phi$  the variation of  $\Omega_R^2$  with increasing  $n_s$  is practically flat at the value corresponding to  $n_s = 0$  (absence of the metallic sheet) up to a point where it changes rapidly, increasing to a maximum and then dropping sharply to a relatively small value at a higher range of  $n_s$ . This feature at large  $n_s$  signifies screening effects. The peak of  $\Omega_R^2$  corresponds to the value of  $n_s$  satisfying the condition  $k_{z1} d = \omega^2 / \Lambda^2$ , which is similar to (but not the same as) the dispersion relation of the surface mode in this system which is [24-26]

$$\frac{k_{z1} d}{\left( \frac{\epsilon_2}{\epsilon_1} + \left[ 1 - \frac{\omega^2}{c^2 k_{z1}^2 d^2} (\epsilon_2 - \epsilon_1) \right]^{1/2} \right)} = \frac{\omega^2}{\Lambda^2} \quad (19)$$

This surface mode, in turn, differs from the usual surface plasmon mode arising on a semi-infinite metallic half space. At an angle of incidence approximately equal to  $\phi_0$  for

total internal reflection, the Rabi frequency exhibits a resonance which is at least two orders of magnitude larger than the value corresponding to the absence of the metallic sheet. At  $\phi = \phi_0$  (not shown in the Fig. 2) the squared Rabi frequency  $\Omega_R^2$  would be in the form of a delta function. In principle, then, pronounced repulsion effects would be expected in conditions corresponding to the region of the resonance.

The real mirror action is only partially influenced by the behaviour of the Rabi frequency; dynamical effects are, of course, controlled by the forces acting on the atomic centre of mass. The atom experiences besides the average radiation force given by Eq.(12), an attractive force due to interaction with the vacuum fields which are constrained by the presence of the surface. At distances from the surface large compared to a reduced transition wavelength  $\lambda_0/2\pi$  the atom-surface force takes the Casimir-Polder form. At distances smaller than  $\lambda_0/2\pi$  the force assumes the van der Waals form. As we show shortly, the important region for the atomic mirrors considered here, is, in fact, the van der Waals regime for which the force can be written as

$$\mathbf{F}_{\text{vw}}(z) = -\frac{\partial U_{\text{vw}}}{\partial z} \quad (20)$$

where  $U_{\text{vw}}$  is the image potential. As is well known, the van der Waals potential arises as the position-dependent change in the radiative self energy due to the presence of the surface, but it depends on the orientation of the electric dipole moment relative to the surface. It should be emphasised that the evanescent field has no other role to play in the determination of the van der Waals potential, except that it is responsible for the dipole orientation. The average electric dipole aligns itself parallel to  $\hat{\mathbf{e}}_1$ , a unit vector in the direction of the local evanescent electric field so that  $\mathbf{E}_1(\mathbf{r}) = \hat{\mathbf{e}}_1 E_1(\mathbf{r})$ . In the field-dipole orientation picture this state of affairs applies at every point along the atom trajectory. The leading contribution to the van der Waals potential arises from the interaction of the electric dipole with its image and we therefore have

$$U_{\text{vw}}(z) = -\frac{\mu^2}{32\pi\epsilon_0 z^3} \left\{ 3(\hat{\mathbf{e}}_1 \cdot \hat{\mathbf{z}})(\tilde{\hat{\mathbf{e}}}_1 \cdot \hat{\mathbf{z}}) - \hat{\mathbf{e}}_1 \cdot \tilde{\hat{\mathbf{e}}}_1 \right\} \quad (21)$$

where the unit vector  $\tilde{\hat{\mathbf{e}}}_1$  is the image of  $\hat{\mathbf{e}}_1$ .

The atomic reflection process is controlled by two separate mechanisms. Firstly, the spontaneous force  $\mathbf{F}_s$  acts on the atom in the direction of  $\mathbf{k}_{\parallel}$  and, secondly, the combined force  $\mathbf{F}_d + \mathbf{F}_{vw}$  acts to repel the atom from the surface, decelerating its motion along the  $z$ -axis towards the surface, attaining an instantaneous halt before changing direction away from the surface at an appropriate turning point in the trajectory. This behaviour can be seen more clearly by examining the corresponding repulsive potential  $U_T(\mathbf{v}, z) = U_{vw}(z) + U_d(\mathbf{v}, z)$  which is shown in Fig. 3 for a typical set of parameters. Note that by controlling the average dipole direction the field-dipole orientation picture influences the variations of both  $U_{vw}$  and  $U_d$ .

The trajectory of the atom of mass  $M$  approaching a mirror for a given set up is obtainable by solving the equation of motion

$$M \frac{d^2 \mathbf{r}}{dt^2} = \mathbf{F}_s + \mathbf{F}_d + \mathbf{F}_{vw} - Mg\hat{\mathbf{z}} \quad (22)$$

subject to given initial conditions. Figure 4 displays typical trajectories in the plane of incidence. The parameters are such that the spontaneous rate  $\Gamma$  is taken to be the free space value  $\Gamma_0$ . This is in fact a very good approximation in the trajectory region which is sufficiently far from the metallic sheet and the substrate. The static detuning is taken to be  $\Delta_0 = 5 \times 10^2 \Gamma_0$ . Finally the intensity of the light is assumed to be  $I = 2.0 \times 10^4 \text{W m}^{-2}$ . It is straightforward to verify that for this light intensity and for the detuning value used here, the saturation parameter  $S = 2\Omega_R^2(0)/(\Delta^2 + \Gamma_0^2) \approx 0.23$  which conforms with the low intensity regime.

In view of Fig. 4 one concludes that the structure operates as an atomic mirror in three of the cases displayed, while for the fourth case the trajectory of the atom terminates with a collision at the surface. An approximate guide to the condition leading to a collision with the surface is to compare the maximum height  $U_{max}$  of the potential in Fig. 3 to the initial kinetic energy  $Mv_z^2(0)/2$ . For  $v_z(0) > \sqrt{2U_{max}/M}$  a collision

occurs. This interpretation indeed conforms with the results of the type shown in Fig. 3. Note that reflected atom trajectories are, in general, asymmetric with respect to the turning point. This is a consequence of the action of  $\mathbf{F}_s$ , which in the present example where the light and the atom are incident on the same side (left side) of the z-axis, accelerates the atom to the right along the surface.

In conclusion, we have explored the influence of adding a metallic sheet to the usual evanescent mode atomic mirror set up. The theory presented provides information about the range of metallic sheet densities and the angle of incidence at which the Rabi frequency exhibits pronounced enhancement effects. We have also adopted the field-dipole orientation picture in which the average atomic dipole oscillates along the direction of the electric field of the evanescent mode at every point in the trajectory. We have seen that this step which allowed us to identify the direction of the average dipole moment vector as that of the local electric field vector at every point in the trajectory, has important consequences for the evaluation of the forces and, hence, the dynamics of the atom. Our results show that enhancement arises at an angle of incidence close to that of the total internal reflection condition, but requires a relatively high sheet density.

**Acknowledgement:**

JBK and CRB are grateful to the EPSRC for financial support. This work has been carried out under the EPSRC grant number GR/M16313

## References

1. V I Cooke and R K Hill, *Opt. Commun.* **43**, 258 (1982)
2. W Seifert, C S Adams, V I Balykin, C Heine, Yu Ovchinikov and J Mlynek, *Phys. Rev.* **A49**, 3814 (1994)
3. G I Opat, S J Wark and A Cimmino, *Appl. Phys.* **B54**, 396 (1992)
4. S Tan and D F Walls, *J. Phys. II (France)* **4**, 1879 (1994)
5. P Ryytty, M Kaivola and C G Aminoff, *Europhys. Lett.* **36**, 343 (1996)
6. R J Wilson, B Holst and W Allison, *Rev. Sci. Instrum* **70**, 2960 (1999)
7. D C Lau, A I Sidrov, G I Opat, R J McLean, W J Rowlands and P Hannaford, *Eur. Phys. J D* **5**, 193 (1999)
8. R Cote, B Segev and M G Raisen, *Phys. Rev.* **A58**, 3999 (1998)
9. L Cagnet, V Savalli, G Zs K Horvath, D Holleville, R Marani, N Westbrook, C I Westbrook and A Aspect, *Phys. Rev. Lett.* **81**, 5044 (1998)
10. H Gauck, M Hartl, D Schneble, H Schnitzler, T Pfau and J Mlynek, *Phys. Rev. Lett.* **81**, 5298 (1998)
11. L Santos and L Rose, *Phys. Rev.* **A58**, 2407 (1998)
12. N Friedman, R Ozeri and N Davidson, *J. Opt. Soc. Am.* **15**, 1749 (1998)
13. P Szriftgiser, D Guery-Odelin, P Desbiolles, J Dalibard, M Arndt and A Steane, *Acta Phys. Pol.* **93**, 197 (1998)
14. J P Dowling and J Gea- Banacloche, *Adv. Atom. Mol. Opt. Phy.* **37**, 1 (1997)
15. A Landragin, J Y Courtois, G Labeyrie, N Vansteenkiste, C I Westbrook and A Aspect, *Phys. Rev. Lett.* **77**, 1464 (1996)

16. N Vansteenkiste, A Landragin, G. Labeyrie, R Kaiser, C I Westbrook and A Aspect, *Ann. Phys.-Paris* **20**, 595 (1995)
17. S M Tan and D F Walls, *Phys. Rev.* **A50**, 1561 (1994)
18. S Feron, J Reinhardt, S Leboutoux, O Gocreix, J Baudon, M Ducloy, J Robert, C Miniatura, S N Chormaic, H Haberland and V Lorent, *Opt. Commun.* **102**, 83 (1993)
19. T Esslinger, M Weidenmüller, A Hammerich and T W Hänych, *Opt. Lett.* **18**, 450 (1993)
20. J P Gordon and A Ashkin, *Phys. Rev.* **A21**, 1606 (1980)
21. J Dalibard and C Cohen-Tannoudji, *J. Phys.* **B18**, 1661 (1985)
22. M Babiker and S Al-Awfi, *Opt. Commun.* **168**, 145 (1999); L Allen, M Babiker, W K Lai and V E Lembessis, *Phys. Rev.* **A54**, 4259 (1996)
23. R Loudon *The Quantum Theory of Light*, 2nd Edn. (Oxford, 1995)
24. F Stern, *Phys. Rev. Lett.* **18**, 546 (1967)
25. A L Fetter, *Ann. Phys. (NY)* **81**, 367 (1973)
26. C R Bennett, J B Kirk, and M Babiker, to be submitted.

## Figure Captions

### Figure 1

Schematic arrangement of the elements comprising an evanescent mode atomic mirror with a metallic sheet. The plane of incidence contains the internally reflected light beam as well as a typical atomic trajectory. Here both the atom and the light are initially propagating on the same side of the vertical (z-axis).

### Figure 2

Variation with areal density  $n_s$  (in units of  $n_s^{silver} = 5.573 \times 10^{18} \text{m}^{-2}$ ) of  $\Omega_R^2$ , the squared evanescent mode Rabi frequency (in arbitrary units), evaluated just outside the metallic sheet in the limit of small  $\gamma$ . The different curves correspond to different angles of incidence  $\phi = 42.00^\circ$  (dashes);  $\phi = 47.00^\circ$  (dash-dots);  $\phi = 52.00^\circ$  (dash-double dots). The inset (solid curve) shows the variation for  $\phi = 41.37^\circ$ , which is very close to the angle  $\phi_0$  for total internal reflection. The parameters are such that  $\epsilon_2 = 2.298$ , corresponding to an angle of total internal reflection  $\phi_0 = 41.27^\circ$ ;  $\Gamma_0 = 6.128 \times 10^6 \text{ s}^{-1}$ ;  $\Delta_0 = 5.0 \times 10^2 \Gamma_0$  and the intensity of the light is taken as  $I = 2.0 \times 10^4 \text{ Wm}^{-2}$  for the Rb resonance at the transition wavelength  $\lambda_0 = 780 \text{ nm}$ . The scaling length  $d$  is taken as  $d = 15 \text{ nm}$ .

### Figure 3

Variation with  $z$  (in units of  $d = 15 \text{ nm}$ ) of the combined static dipole potential  $U = U_d + U_{vw}$  acting on a Rb atom (in units of  $\hbar\Gamma_0/2$ ). The curves correspond to a fixed value of  $n_s = 215n_s^{silver}$ , but different values of angle of incidence  $\phi$ . They are as follows:  $\phi = 42.00^\circ$  (dashes);  $\phi = 45.00^\circ$  (dash-dots);  $\phi = 47.00^\circ$  (dash-double dots);  $\phi = 41.37^\circ$  (solid curve). The dotted curve shows the variation of the van der Waals potential. In

the evaluation of the potentials, the direction of the dipole moment vector conforms with the field-dipole orientation picture. The parameters are the same as those used in the evaluation of Fig. 2.

#### Figure 4

Atomic trajectories of a Rb atom in the atomic mirror arrangement shown in Fig.1 with the x-z plane as the plane of incidence. The angle of incidence is fixed at  $\phi = 42.00^\circ$  and the metallic sheet corresponds to  $n_s = 215n_s^{silver}$ , as in Fig. 3. In all cases the initial position of the atom is at the point  $(x = 0, z = 100d)$ , where  $d = 15\text{nm}$ . The different trajectories correspond to the same initial condition for the horizontal component of the velocity  $v_{\parallel}(0) = 0.054 \text{ ms}^{-1}$ , but differ in their initial z-component of velocity  $v_z(0)$ . They are as follows:  $v_z(0) = 0.1\text{ms}^{-1}$  (solid curve);  $v_z(0) = 0.4\text{ms}^{-1}$  (dashed curve);  $v_z(0) = 0.7\text{ms}^{-1}$  (dash-dotted curve);  $v_z(0) = 1.1\text{ms}^{-1}$  (dash-double dotted curve). The parameters are the same as those in Figs. 2 and 3.

Figure 1

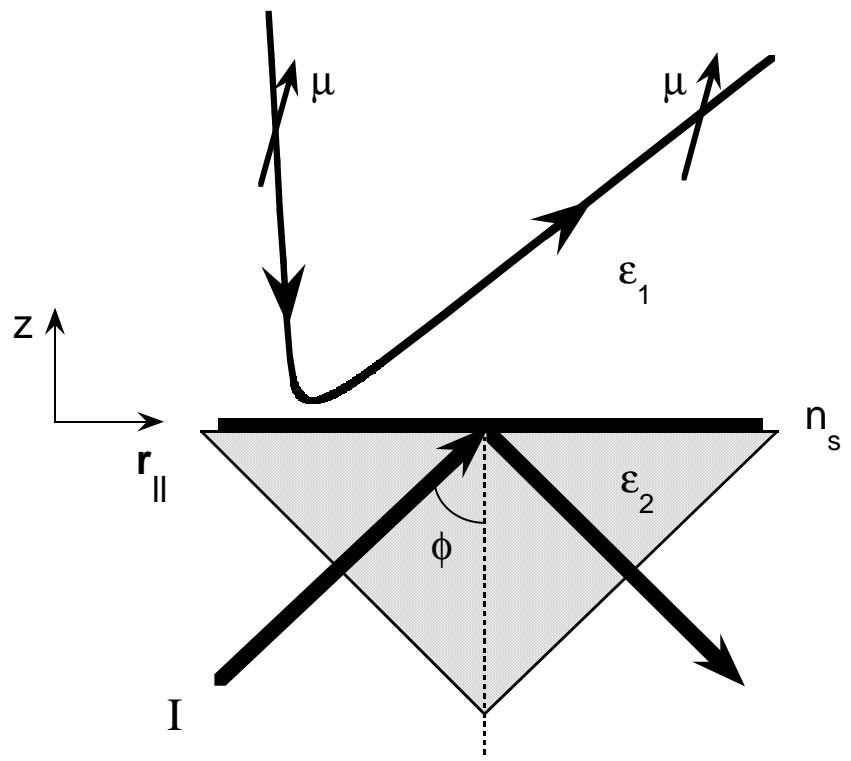


**Figure 2**

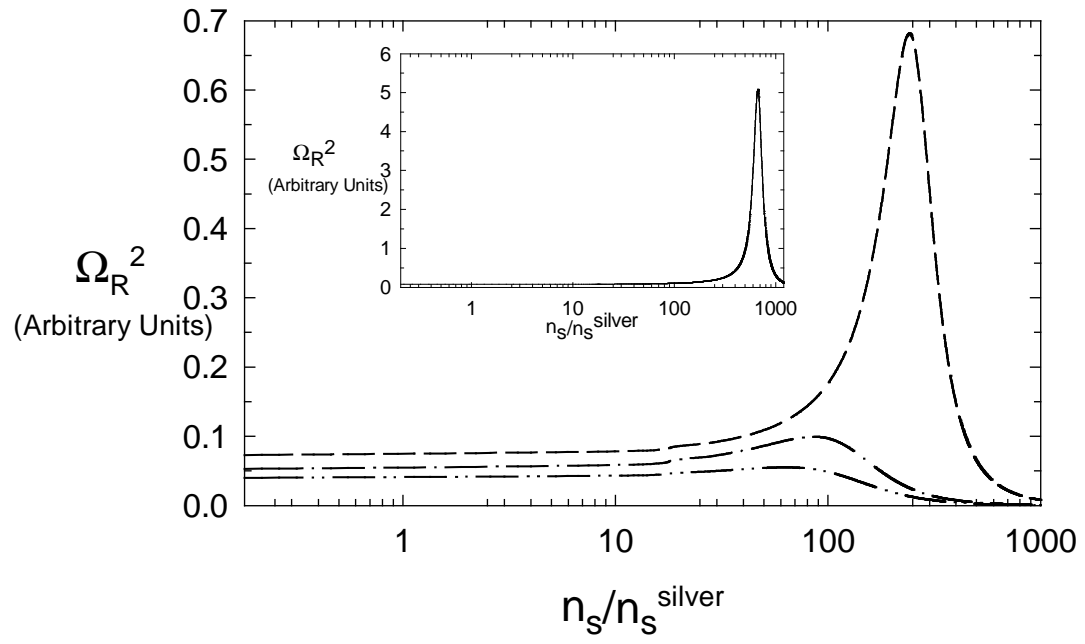


**Figure 3**

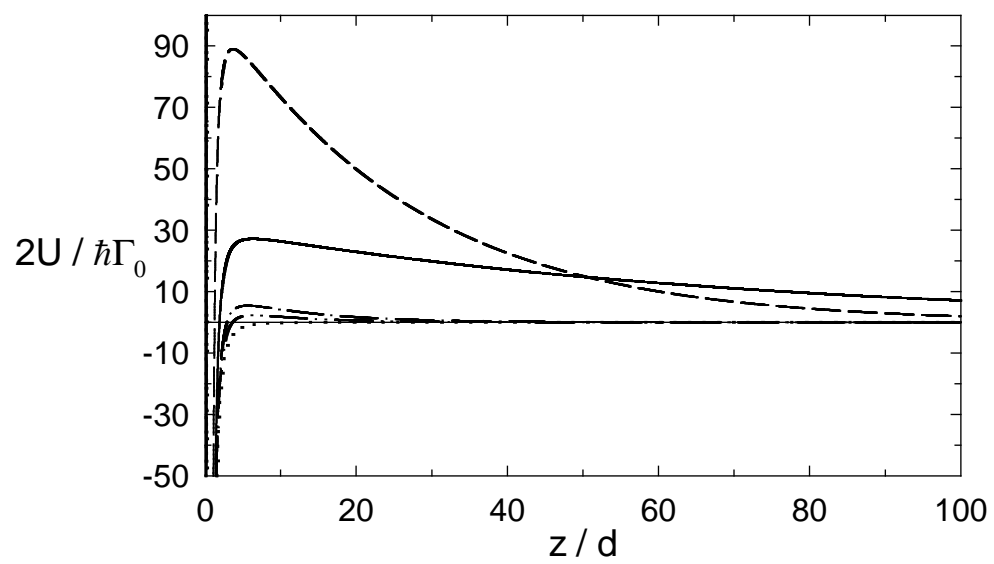


**Figure 4**

